Electrical characteristics of metal–insulator–semiconductor Schottky diodes using a photowashing treatment in Al x Ga 1−x As/InGaAs (X=0.75) pseudomorphic high electron mobility transistors

Sang Youn Han, Kyoung Jin Choi, Jong-Lam Lee, Jae Kyoung Mun, Min Park, and Haechon Kim

Articles you may be interested in

Electrical characteristics of metal–insulator–semiconductor Schottky diodes using a photowashing treatment in $Al_xGa_{1-x}As$/InGaAs ($X=0.75$) pseudomorphic high electron mobility transistors

Sang Youn Han, Kyoung Jin Choi, and Jong-Lam Lee[a)]
Department of Materials Science and Engineering, Pohang University of Science and Technology (POSTECH), Pohang, Kyungbuk 790-784, Korea

Jae Kyoung Mun, Min Park, and Haechon Kim
Microwave Devices Team, Basic Research Laboratory, Electronics and Telecommunications Research Institute (ETRI), Daejeon 305-350, Korea

Metal–insulator–semiconductor (MIS) Schottky diodes on $Al_{0.75}Ga_{0.25}As$/$In_{0.2}Ga_{0.8}As$ pseudomorphic high electron mobility transistors were produced using both photowashing and H_2O_2 treatments. The Schottky contact on a GaAs layer showed enhancement of the Schottky barrier height of 0.11 eV for the photowashing and 0.05 eV for the H_2O_2 treatment, respectively. After the photowashing treatment, the Ga oxide (Ga_2O_3) was dominantly created. In the meanwhile, two types of As oxide (As_2O_3, As_5O_2) were mainly produced by the H_2O_2 treatment, which were distributed uniformly over the GaAs surface. At the same oxide thickness, the formation of the Ga oxide after the photowashing treatment is more effective in enhancement of the Schottky barrier height. This is due to the fact that the Ga oxide was more favorable in the creation of a fixed interface state density, which is known as an origin for increase of the barrier height, compared to the As oxide in the GaAs MIS Schottky diode. © *2003 American Vacuum Society.* [DOI: 10.1116/1.1612514]

I. INTRODUCTION

AlGaAs/InGaAs pseudomorphic high electron mobility transistors (PHEMTs) have attracted a great deal of attention for their outstanding microwave performance because of their superior transport properties. When the Al content in AlGaAs layers increases (>0.7), the energy level of the *DX* centers becomes nearer to the conduction-band edge than that of shallow donors, and thus *DX* centers are known to have little effect on electrical properties. In addition, the Schottky barrier height (SBH) and conduction-band offset between the AlGaAs and InGaAs channels can be increased by adopting an AlGaAs layer with high Al mole fraction, resulting in decrease of the gate leakage current and enhancement of the carrier confinement in the two-dimensional electron gas (2DEG), respectively.[1] These good properties enable us to realize enhancement-mode PHEMTs, which can be operated without negative gate voltage, leading to reduction of the size and cost of the end product.

The SBH of the gate contact is one of the most important parameters of the devices. A high barrier height improves the transconductance and breakdown voltage of electronic devices, leading to the increase of power performance. Of recent years, tuning of the SBH in a quite interval has been achieved via an ultrathin semiconductor[2,3] or insulator interlayer beneath the Schottky contact.[4–8] Among them, many attempts have been made to realize the modification of the SBH using a thin oxide or insulator.[4–6] The insulating inter-

layer of the deposited SiO_2 and native oxide has been used in the development of a better dielectric layer on the III–V semiconductor surface. The enhancement in SBH has been explained by several models such as the increase in fixed negative charge,[9] trapping/chemical interaction,[10] and tunneling/hopping effect,[11] but the underlying mechanism is not yet resolved. Besides, the metal–insulator–semiconductor (MIS) structures reported were not successful, due to a high density of defects and difficulty in achieving a very thin insulating layer without pin holes.[11,12]

Recently, it was reported that dipping GaAs wafers in deionized water under an intense light source (photowashing treatment) resulted in linear growth of an oxide layer, reducing the surface state density and unpinning of the surface Fermi level. This method is convenient and effective in producing thin insulating oxide layers on the GaAs surface.[13–16] However, to our knowledge, no work has been conducted for the fabrication of MIS Schottky diodes using the photowashing treatment. In addition, the relation between the type of oxides created and their electrical properties in MIS Schottky diodes has not been reported.

In the present work, we investigated the electrical properties of MIS Schottky diodes on undoped GaAs and AlGaAs layers, respectively. Both photowashing and the H_2O_2 treatments were adopted for production of thin oxide layers. Synchrotron radiation photoemission spectroscopy (SRPES) was employed for analysis of the chemical composition of the produced oxides. From these, the underlying mechanism for the change of electrical characteristics is proposed.

[a)]Electronic mail: jllee@postech.ac.kr

| Undoped GaAs Cap Layer (40 nm) |
| Undoped n-Al$_{0.75}$Ga$_{0.25}$As (25 nm) |
| Si planar doping, 1.0×10^{12} /cm^2 |
| Undoped Al$_{0.75}$Ga$_{0.25}$As Spacer (3 nm) |
| Undoped In$_{0.2}$Ga$_{0.8}$As Channel (10 nm) |
| Undoped Al$_{0.75}$Ga$_{0.25}$As Spacer (3 nm) |
| Si planar doping, 3.0×10^{12} /cm^2 |
| Undoped Al$_{0.75}$Ga$_{0.25}$As (50 nm) |
| Al$_{0.23}$Ga$_{0.77}$As 5 nm/GaAs 5 nm Superlattice (30 periods) |
| Undoped GaAs Buffer (500 nm) |
| Semi-insulating GaAs Substrate |

F$_{IG}$. 1. Schematic cross-sectional view of an Al$_{0.75}$Ga$_{0.25}$As/InGaAs PHEMT structure used in this study.

II. EXPERIMENTAL PROCEDURES

Figure 1 shows the cross-sectional diagram of an Al$_{0.75}$Ga$_{0.25}$As/In$_{0.2}$Ga$_{0.8}$As PHEMT grown by molecular beam epitaxy on a 4 in. semi-insulating GaAs substrate. The buffer layers consist of a 500-nm-thick undoped GaAs layer and a 30 period undoped Al$_{0.23}$Ga$_{0.77}$As/GaAs superlattice. The active part of the structure is a 10-nm-thick In$_{0.2}$Ga$_{0.8}$As channel sandwiched between upper and lower 3-nm-thick Al$_{0.75}$Ga$_{0.25}$As spacer layers. 2DEG is formed in the pseudomorphic InGaAs channel by electron transfer from the upper and lower silicon-planar-doped layers with a density of 1 $\times 10^{12}$ and 3×10^{12}/cm^2, respectively. An undoped Al$_{0.75}$Ga$_{0.25}$As layer was grown on the planar-doped layer for the Schottky contact. Undoped GaAs (40 nm thick) was used as a cap layer.

An active region was defined by an etching solution of H$_3$PO$_4$: H$_2$O$_2$: H$_2$O. Ohmic metals, Au/Ge/Ni/Au (53 nm/46 nm/30 nm/100 nm), were deposited by an electron-beam evaporator under a base pressure of 5×10^{-7} Torr, followed by postannealing at 420 °C for 1 min. The typical value of the specific contact resistivity was about 2×10^{-6} Ω cm^2, measured using the transfer length method (TLM). In order to investigate the dependence of the epilayer, one set was treated on an undoped GaAs cap layer and the other was treated on an etched AlGaAs layer. The undoped GaAs cap layer was etched using an etching solution of H$_3$PO$_4$: H$_2$O$_2$: H$_2$O.

Production of the oxide layer was performed using both photowashing and H$_2$O$_2$ treatments. The photowashing treatment was performed by dipping the sample in deionized water under an intense Xe lamp for 10 min. Also, the H$_2$O$_2$ treatment was conducted by dipping in dilute H$_2$O$_2$ solution (H$_2$O$_2$: H$_2$O = 1 : 3, H$_2$O$_2$ treatment) for 3 min. Then, the gate metals, Ti/Pt/Au (30 nm/20 nm/50 nm), were deposited on the oxidized layer.

The chemical compositions at the surfaces of the GaAs and AlGaAs layers were characterized using SRPES measurements at the 4B1 beam line in the Pohang Accelerator Laboratory (PAL). The incident photon energy of 400 eV,
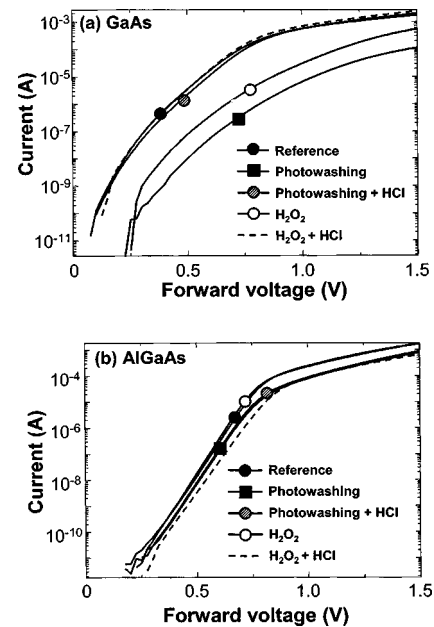

FIG. 2. Forward current–voltage ($I-V$) characteristics of the Ti/Pt/Au Schottky contacts with the type of surface oxidation treatments on the (a) GaAs and (b) AlGaAs layers.

which is sensitive in the measurement of surface components, was used to obtain Ga 3d and As 3d core level spectra. The incident photon energy was calibrated with the core level spectrum of Au 4f and the energy step in the measurement was 0.05 eV.

III. RESULTS

A. Electrical characteristics

The current–voltage ($I-V$) characteristics of the Ti/Pt/Au Schottky contact on the undoped GaAs and AlGaAs layers as a type of oxidation treatments are shown in Figs. 2(a) and 2(b). Under thermionic emission of electrons from the metal to semiconductor with low doping concentration, the $I-V$ characteristics could be expressed as[17]

$$I = AA^*T^2 \exp\left(-\frac{q\phi_b}{kT}\right)\left[\exp\left(\frac{qV}{nkT}\right) - 1\right], \quad (1)$$

where A is the device area and A^* the effective Richardson constant, n the ideality factor, and $q\phi_b$ the effective SBH. The values of $q\phi_b$ and n were determined from the intercept and the slope of the linear region in the plot of ln(I) vs V, which are summarized in Table I.

In the Schottky contact formed on the undoped GaAs cap layer, the SBH of photowashing treated MIS Schottky diode increased from 0.79 to 0.9 eV in comparison with the reference device (no oxidation treatment). However, the ideality factor after photowashing significantly increased. This implies that another current transport mechanism is involved at the metal/GaAs interface. A large deviation from the ideal value could be attributed to the surface oxide layer with different thicknesses and to the interface states which are in equilibrium with the semiconductor as reported

TABLE I. Schottky barrier height (ϕ_B) and ideality factor (η) for both photowashing-treated and H$_2$O$_2$-treated samples.

Treatment	GaAs		AlGaAs	
	ϕ_B (eV)	η	ϕ_B (eV)	η
Reference	0.79	1.32	0.96	1.25
Photowashing	0.90	1.86	0.97	1.29
Photowashing + HCl	0.77	1.43	0.95	1.27
H$_2$O$_2$ treatment	0.84	1.79	0.96	1.23
H$_2$O$_2$ treatment + HCl	0.74	1.58	0.97	1.37

previously.[10,18] After the oxide created on the surface was etched off by HCl solution, the values of the SBH and ideality factor returned to that of the reference device. This indicated that increase of the SBH originated from the surface oxide layer produced by the photowashing treatment. Also, in the H$_2$O$_2$-treated diode, the SBH increase by 0.05 eV with the H$_2$O$_2$ treatment. As observed in the photowashing treated sample, the SBH of the H$_2$O$_2$ treated one decreased to the value of the reference device, when the oxide layer was etched off.

In the Schottky contact formed on the undoped AlGaAs layer, however, no further improvement in the SBH was found. This could be interpreted by the larger Gibbs free-energy change in the formation of Al$_2$O$_3$ (-1560 kJ/mol) (Ref. 19) at room temperature. Therefore, an Al oxide can be easily formed on the AlGaAs surface, resulting in suppression of growth of the oxide layer by the photowashing and H$_2$O$_2$ treatments.

B. Microstructural analysis by SRPES

Figure 3(a) shows SRPES spectra of the Ga $3d$ core level with the type of surface oxidation and deoxidation process. The Ga $3d$ peak could be separated into two bonds with binding energies of 19.4 and 21.0 eV, corresponding to Ga–As and Ga–O bonds, respectively. The binding energy differences of ~ 1.6 eV ($= E_{Ga-O} - E_{Ga-As}$) are in good agreement with previously reported values.[20–23] After the photowashing treatment, the intensity of the Ga–O bond drastically increased, but the peak for the Ga–As bond nearly disappeared. This indicated that photowashing is effective in producing the surface oxide layer. However, the Ga–As bond appeared when dipped in HCl solution. In the H$_2$O$_2$ treatment, the intensity of the Ga–O bond increased, as observed in the photowashing treated sample.

Figure 3(b) shows SRPES spectra of the As $3d$ core level with the type of surface treatment. At the as-deposited state, the As $3d$ peak could be separated into two bonds, corresponding to As–Ga, and As–As (metallic) bonds, respectively. After the photowashing treatment, two peaks for As–Ga and the As–O (As$_2$O$_3$) were observed and the binding energy difference was ~ 3.8 eV, consistent with previous reports.[21–24] The peak intensity of the As–O bond increased drastically. In the meanwhile, the driving force for both As$_2$O$_3$ and As$_5$O$_2$ formation is quite large, i.e., ΔG_f^0 values at 298 K are -576 and -772 kJ/mol for As$_2$O$_3$ and As$_5$O$_2$,

respectively, indicating that formation of As$_5$O$_2$ is thermodynamically preferred.[19,20] However, only As$_2$O$_3$ is formed after the photowashing treatment. In the H$_2$O$_2$ treatment, the As $3d$ peak could be separated into three bonds with binding energies of 41.7, 45.2, and 46.4 eV, corresponding to As–Ga, As–O (As$_2$O$_3$), and As–O (As$_5$O$_2$) bonds, respectively. Compared with the photowashing treated sample, the formation of As$_5$O$_2$ was newly observed in the H$_2$O$_2$ treated one.

The ratio of the substrate to oxide peaks enables calculation of the total oxide thickness. Thus, the oxide film thickness (d) on GaAs is determined from the following expression:[24]

$$d = \lambda \sin \theta \ln(1+L), \tag{2}$$

$$L = \frac{\Sigma_i [I_i(\text{ox})/S_i]}{\Sigma_i (I_i/S_i)}, \tag{3}$$

where λ is the photoelectron mean-free path in the oxide (4 nm), θ the take-off angle (90°), I_i the peak intensity due to
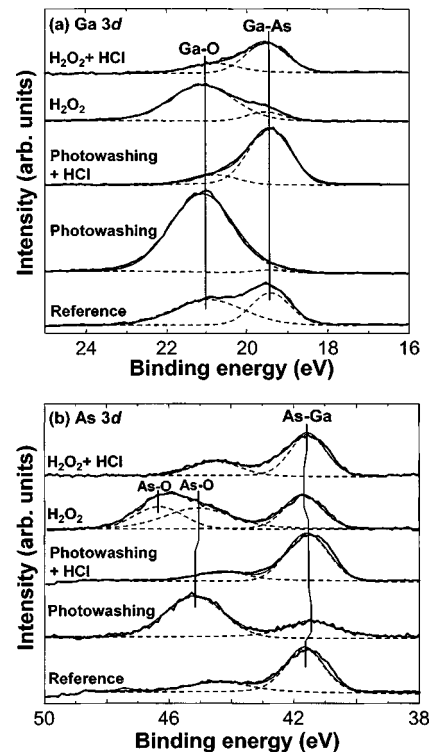

FIG. 3. SRPES spectra with the type of surface oxidation treatments on the GaAs layer: (a) Ga $3d$ core levels and (b) As $3d$ core levels.

TABLE II. Relative atomic concentrations (%) on the GaAs surface with the type of surface oxidation treatments. The thickness of the oxide layer was calculated by the ratio of the substrate to oxide peaks.

	Ga		As		O	C	Thickness (Å)
	Ga–As	Ga–O	As–Ga	As–O			
Reference	4.7	8.0	17.7	4.6	30.2	34.8	12.2
Photowashing	0.4	18.7	4.7	9.4	45.7	21.1	24.3
Photowashing + HCl	9.2	1.7	30.4	6.6	22.6	29.5	6.3
H_2O_2 treatment	1.1	7.3	6.1	12.9	43.0	29.6	22.2
H_2O_2 treatment + HCl	2.6	1.3	7.9	5.3	41.6	41.3	12.8

the substrate, S_i the relative sensitivity, and $I_i(ox)$ the peak intensity due to the oxide. Using this method, the thickness of the oxide on the photowashing treated sample is estimated as 2.4 nm. Likewise, the thickness of the H_2O_2-treated sample is about 2.2 nm, as summarized in Table II. Since the thickness of the oxide layer formed by both treatments was nearly same, the difference in the enhancement of the SBH cannot be attributed to the oxide thickness.

The atomic concentrations of each element were determined using the integral peak intensities and the corresponding atomic sensitivity factors. Based on these, the relative atomic concentrations of the photowashing and H_2O_2-treated samples could be evaluated, and are summarized in Table II. After the photowashing treatment, the formation of Ga oxide is more pronounced than that of As oxide. This could be explained by the washing away of the soluble As oxide in deionized water during the photowashing treatment. Thus, the oxide is primarily composed of Ga_2O_3 with a small amount of As_2O_3. However, after the H_2O_2 treatment, as shown in Table II, the As oxide is dominantly produced. This suggested that the type of oxide layer and/or oxide growth method could be related to the change of electrical characteristics.

In order to obtain depth information of the chemical compositions below the GaAs surface, SRPES measurements were performed as a function of the take-off angle, as shown in Fig. 4. At a small angle, the intensity of photoelectrons emitted from the surface becomes dominant due to the limited inelastic mean-free path of photoelectrons. As the take-off angle was decreased, the intensity of the As–O bonds increased compared with that of the As–Ga one. This indicated that the oxide layer exists at the near-surface region. Figure 4(b) shows the As $3d$ photoelectron spectra of the H_2O_2-treated sample as a function of take-off angle. This informs us that two different types of As oxide formed by the H_2O_2 treatment were distributed uniformly on the GaAs surface.

IV. DISCUSSION

A simple but representative model was proposed to explain the increase in SBH caused by the oxide layer in GaAs MIS Schottky diodes.[9,25] According to this model, the increase in SBH is brought about by a fixed negative charge (for *n*-type semiconductors) at the oxide–semiconductor interface, which partially compensates the positive ionized do-

nor in the semiconductor space charge region. This tends to reduce the net charge in the metal and to reduce the oxide potential drop (Δ). For the constant metal work function and semiconductor electron affinity, this implies an increase in SBH compared to the case where the oxide thickness is zero, i.e., with an intimate metal–semiconductor (MS) contact. By a simple application of Gauss's law, the increase in barrier height caused by the oxide layer and the negative interfacial charge has been shown to be

$$\Delta\phi_B = \frac{Q_{ss}}{2\varepsilon_i}\delta, \tag{4}$$

where $\Delta\phi_B$ is the increase in SBH by formation of an oxide layer between the MS, Q_{ss} the fixed negative charge density at insulator/semiconductor interface, δ the thickness of oxide layer, and ε_i the permittivity of the oxide insulator.
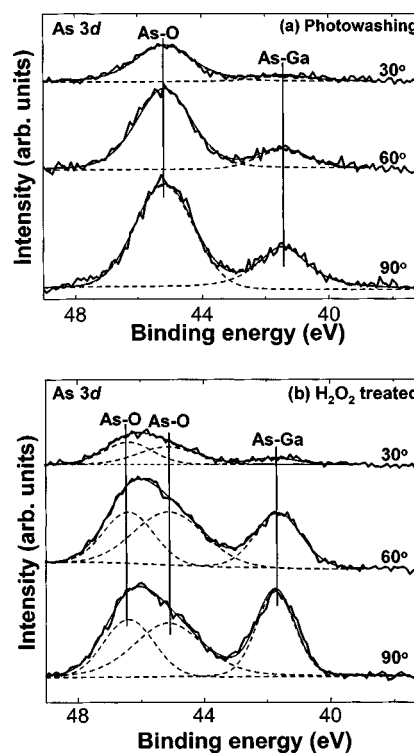

FIG. 4. As $3d$ core levels photoemission spectra as a function of take-off angle between the GaAs surface and the trajectory of emitted electrons in (a) photowashing treated and (b) H_2O_2 treated samples.

According to the $I-V$ characteristics, enhancement of the SBH by photowashing is more pronounced than that by the H_2O_2 treatment, as shown in Fig. 1 and Table I. From Table II, the Ga oxide is mainly produced by the photowashing treatment, meanwhile two types of As oxide are dominantly created by the H_2O_2 treatment, which are distributed uniformly over the surface. Our experimental results were applied to the above model. Since the thickness of the oxide layer formed by both treatments was nearly the same, the difference in the enhancement of the SBH can be attributed to the fixed negative charge density at the insulator/semiconductor interface (Q_{ss}), and the fixed negative charge densities by the photowashing and H_2O_2 treatments could be estimated to be 1.75×10^{12} and 8.72×10^{11} cm^{-2}, respectively. Consequently, the photowashing treatment is more favorable in creation of the fixed interface state density (Q_{ss}) and it is expected that the fixed interface state density could be related to the oxide growth method and oxide quality.

V. CONCLUSION

In conclusion, MIS Schottky diodes on $Al_{0.75}Ga_{0.25}As/In_{0.2}Ga_{0.8}As$ PHEMTs were produced using both photowashing and H_2O_2 treatments. The Schottky contact on the GaAs layer with photowashing and H_2O_2 treatments showed enhancements of the SBH of about 0.11 and 0.05 eV, respectively. However, on the undoped AlGaAs layer, no further improvement in SBH was observed. After the photowashing treatment, the Ga oxide (Ga_2O_3) was dominantly created. In the meanwhile, two types of As oxide (As_2O_3, As_5O_2) were mainly produced by the H_2O_2 treatment, which are distributed uniformly on the GaAs surface. The thickness of the oxide layer formed by both treatments was nearly the same. Applying a representative model, formation of Ga oxide after the photowashing treatment is effective in enhancement of the SBH. This is due to the fact that the Ga oxide was more favorable in creation of the fixed interface state density, which is known as an origin for increase of the barrier height, compared to As oxide in the GaAs MIS Schottky diode.

ACKNOWLEDGMENTS

[1]Motorola: Compound Semiconductor **6**, 28 (2001).

[2]J. Ivanco, H. Kobayashi, J. Almeida, and G. Margaritondo, J. Appl. Phys. **87**, 795 (2000).

[3]T. U. Kampen, S. Park, and D. R. T. Zahn, Appl. Surf. Sci. **190**, 461 (2002).

[4]M. K. Hudait and S. B. Krupanidhi, Solid-State Electron. **44**, 1089 (2000).

[5]A. F. Ozdemir, A. Kokce, and A. Turut, Appl. Surf. Sci. **191**, 188 (2002).

[6]T. Sugimura, T. Tsuzuku, T. Katsui, Y. Kasai, T. Inokuma, S. Hashimoto, K. Iiyama, and S. Takamiya, Solid-State Electron. **43**, 1571 (1999).

[7]M.-J. Jeng, H.-T. Wang, L.-B. Chang, Y.-C. Cheng, and S.-T. Chou, J. Appl. Phys. **86**, 6261 (1999).

[8]C. J. Huang, J. Appl. Phys. **89**, 6501 (2001).

[9]M. Peckerar, J. Appl. Phys. **45**, 4652 (1974).

[10]H. C. Card and E. H. Rhoderick, J. Phys. D **4**, 1589 (1971).

[11]S. Ashok, J. M. Norrego, and R. J. Gutmann, Solid-State Electron. **22**, 621 (1979).

[12]R. B. Childs, J. M. Ruths, T. E. Sullivan, and S. J. Fonash, J. Vac. Sci. Technol. **15**, 1397 (1978).

[13]K. J. Choi, J.-L. Lee, J. K. Mun, and H. Kim, J. Vac. Sci. Technol. B **20**, 274 (2002).

[14]Y. Hirota, J. Appl. Phys. **75**, 1798 (1995).

[15]K. J. Choi, J. K. Mun, M. Park, H. Kim, and J.-L. Lee, Jpn. J. Appl. Phys., Part 1 **41**, 2894 (2002).

[16]D. Kirchner, A. C. Warren, J. M. Woodall, C. W. Wilmsen, S. L. Wright, and J. M. Baker, J. Electrochem. Soc. **135**, 1822 (1988).

[17]E. H. Rhoderick and R. H. Williams, *Metal–Semiconductor Contacts* (Clarendon, Oxford, UK, 1988), p. 38.

[18]M. A. Ebeoglu, F. Temurtas, and Z. Z. Ozturk, Solid-State Electron. **42**, 23 (1998).

[19]Barin Ihsan, *Thermochemical Data of Pure Substances* (VCH, Berlin, 1987), p. 49.

[20]Z. H. Lu, B. Bryskiewicz, J. McCaffrey, Z. Wasilewski, and M. J. Graham, J. Vac. Sci. Technol. B **11**, 2033 (1993).

[21]C. C. Surdu-Bob, S. O. Saied, and J. L. Sullivan, Appl. Surf. Sci. **183**, 126 (2001).

[22]D. Ghidaoui, S. B. Lyon, G. E. Thompson, and J. Walton, Corros. Sci. **44**, 501 (2002).

[23]J. F. Moulder, W. F. Stickle, P. E. Sobol, and K. D. Bomben, *Handbook of X-Ray Photoelectron Spectroscopy* (Perkin-Elmer, Eden Prairie, MN, 1992), p. 179.

[24]M. F. Hochella, Jr., and A. H. Carim, Surf. Sci. Lett. **197**, L260 (1988).

[25]B. R. Pruniaux and A. C. Adams, J. Appl. Phys. **43**, 1980 (1972).